

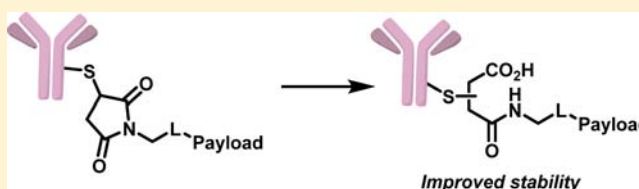
# Mild Method for Succinimide Hydrolysis on ADCs: Impact on ADC Potency, Stability, Exposure, and Efficacy

L. Nathan Tumey,<sup>\*,†</sup> Manoj Charati,<sup>||</sup> Tao He,<sup>‡</sup> Eric Sousa,<sup>‡</sup> Dangshe Ma,<sup>||</sup> Xiaogang Han,<sup>§</sup> Tracey Clark,<sup>§</sup> Jeff Casavant,<sup>†</sup> Frank Loganzo,<sup>||</sup> Frank Barletta,<sup>§</sup> Judy Lucas,<sup>||</sup> and Edmund I. Graziani<sup>†</sup>

<sup>†</sup>Worldwide Medicinal Chemistry, <sup>‡</sup>Global Biological Technologies, <sup>§</sup>Pharmacokinetics, Metabolism, and Distribution, and <sup>||</sup>Oncology Research Unit, Pfizer Global R&D, Groton, Connecticut 06340, United States

## Supporting Information

**ABSTRACT:** The stability of the connection between the antibody and the toxin can have a profound impact on ADC safety and efficacy. There has been increasing evidence in recent years that maleimide-based ADCs are prone to payload loss via a retro-Michael type reaction. Herein, we report a mild method for the hydrolysis of the succinimide-thioether ring which results in a “ring-opened” linker. ADCs containing this hydrolyzed succinimide linker show equivalent cytotoxicity, improved *in vitro* stability, improved PK exposure, and improved efficacy as compared to their nonhydrolyzed counterparts. This method offers a simple way to improve the stability, exposure, and efficacy of maleimide-based ADCs.



## INTRODUCTION

Antibody–drug conjugates (ADCs) have become increasingly recognized as an important modality for the treatment of cancer. This is clearly reflected in increased industrial R&D activities,<sup>1</sup> an expanding clinical pipeline,<sup>2</sup> and two recently approved drugs.<sup>3</sup> ADCs combine the exquisite selectivity of biological ligands (antibodies) with the pronounced potency of small molecule toxins. The stability of the connection between the antibody and the toxin can have a profound impact on ADC safety and efficacy. Premature cleavage of the toxin from the antibody results in two potential issues: (1) systemic exposure of nontargeted toxins may adversely affect the safety of the ADC and (2) the remaining ADC in circulation may have reduced efficacy due to lower concentration of conjugated toxin. This issue has been recognized since the earliest days of ADC research, and in fact, linker stability was a major factor in the selection of the specific hydrazone linkage used in the first marketed ADC (Mylotarg).<sup>4</sup> In spite of these efforts, studies have shown that Mylotarg and the related ADC CMC-544 lose payload in plasma, presumably due to slow hydrolysis of the hydrazone linkage.<sup>5</sup> Movement away from hydrazone linkages does not completely ameliorate this problem. Disulfide-linked ADC huC242-SPP-DM1 was found to lose significant amounts of payload during circulation, as evidenced by the 3× higher total payload clearance than the total antibody clearance for this ADC.<sup>6</sup>

Thioethers formed by the reaction of maleimide electrophiles with endogenous and engineered cysteine residues were initially thought to circumvent some of the above stability issues. However, it has been demonstrated that the auristatin-based linker-payload (LP) maleimide caproyl monomethyl auristatin F (mcMMAF) was slowly transferred from cysteines of an anti-CD70 ADC to the cys-34 residue of serum albumin, losing

approximately 75% of its linker-payload in the time course of the study. The transfer could be blocked by preparing the conjugate using bromoacetamide (bac) chemistry in place of the maleimide chemistry, resulting in an ADC that maintained its drug–antibody ratio (DAR) over the course of a two-week PK study. In spite of the improved stability, minimal improvement in efficacy and no change in the maximum tolerated dose (MTD) was observed, leading the authors to speculate that improvement of the linker half-life beyond the ADC half-life is unlikely to significantly improve overall exposure, and therefore have a minimal effect on efficacy.<sup>7</sup>

Recent experimentation to further illuminate the mechanism of maleimide transfer generated evidence that the succinimide-thioether (A) is in slow equilibrium with the corresponding free maleimide (B)<sup>8</sup> (Figure 1). An exogenous thiol nucleophile can then “capture” the maleimide resulting in formal transfer of the linker-payload (C). The high relative concentration of exogenous nucleophiles (X-SH) such as cysteine, glutathione, and serum albumin serves as an “electrophile sink” which slowly drives down the loading of the maleimide bioconjugate over the ~two week period of ADC exposure. Over the same time frame, the succinimide-thioether is being slowly hydrolyzed to the ring-opened form (D). This hydrolyzed succinimide is not subject to the retro-Michael type mediated loss of payload presumably due to the increased  $pK_a$  of the acid enolate as compared to the succinimide enolate. The relatively slow rate of this succinimide hydrolysis and maleimide-transfer means that its impact will be minimal on ADCs which have high  $T_{ab}$  (total antibody) clearance, while it will be much more

**Received:** August 4, 2014

**Revised:** September 9, 2014

**Published:** September 12, 2014

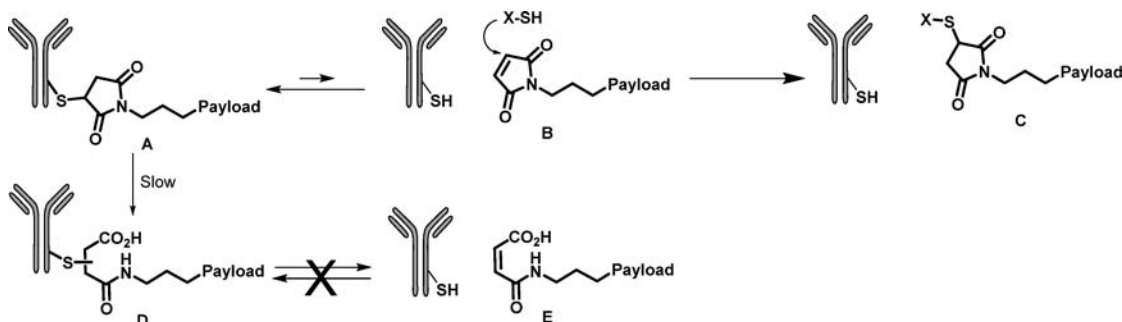


Figure 1. Mechanism for the improved stability of ring-opened succinimides.

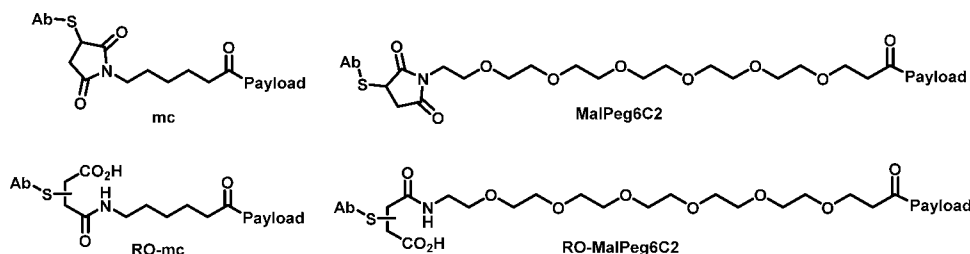
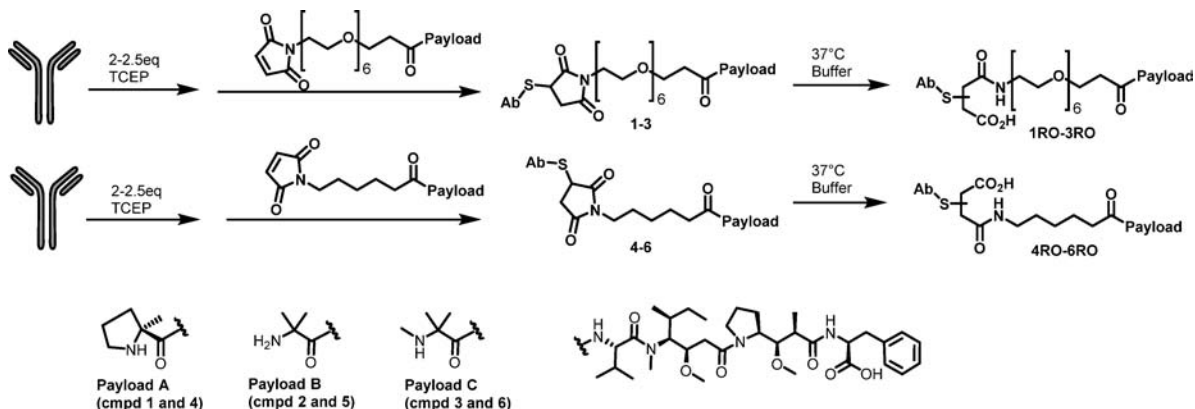


Figure 2. Structure of linkers.

### Scheme 1. Synthesis of Ring-Opened ADCs 1RO–6RO



pronounced on ADCs that are retained in the bloodstream for long periods of time. In short, this means that “ADC clearance” is dictated by two factors: (1) total antibody ( $T_{ab}$ ) clearance and (2) linker cleavage. In some cases, linker cleavage may not be the exposure determining factor, while in other cases it may play a significant role in ADC exposure and, therefore, efficacy.

This is clearly illustrated in a recent publication in which site-specific conjugation to cysteine afforded a series of ADCs that showed varying degrees of spontaneous succinimide hydrolysis, and therefore varying degrees of deconjugation.<sup>9</sup> In contrast to the previous study of bac-linkers,<sup>7</sup> the ADCs with improved stability were observed to have significantly improved efficacy. In light of these studies, we herein describe a method for the intentional succinimide ring hydrolysis of conventional (hinge) conjugated ADCs. The ring-opened ADCs were evaluated in various *in vitro* and *in vivo* studies and were shown to exhibit equivalent *in vitro* potency, improved *in vitro* stability, improved PK exposure, and improved efficacy as compared to their nonhydrolyzed counterparts.

## RESULTS

During the course of studying various ADC payloads, a maleimide linker containing six polyethylene glycol units (MalPeg6C2, Figure 2) was observed to impart modestly improved efficacy and exposure as compared to the corresponding maleimidocaproyl (mc)-linked ADCs (data not shown). Unexpectedly, ADCs incorporating this MalPeg6C2 linker were observed to slowly hydrolyze upon storage in a neutral buffer, resulting in the ring-opened succinimide form of the ADC shown in Figure 2. In contrast, the corresponding mc-linked ADCs did not show any appreciable ring-opening during storage. Based on the previously mentioned reports,<sup>7,9</sup> we reasoned that the propensity of this MalPeg6C2 linker to undergo hydrolysis resulted in the formation of a more stable conjugate. We hypothesized that the improved stability of this linkage was driving the aforementioned improvement in exposure and efficacy. We believe that the susceptibility of the MalPeg linker toward hydrolysis is the result of coordination of a water molecule to the proximal PEG-oxygen, placing it in just the right geometry for addition to the carbonyl. In fact, during the preparation of this manuscript a similar (but

more dramatic) effect was reported when a basic amine was incorporated into the mc-linker.<sup>15c</sup>

**Preparation and Characterization of Hydrolyzed Succinimide Linked ADCs.** This hypothesis led us to develop a plan to intentionally open the maleimide ring in order to specifically probe the improved ADC stability imparted by ring-opening. Following well-established precedent,<sup>10</sup> the anti-Her2 monoclonal antibody (mAb) trastuzumab was reduced with 2–2.5 equiv of TCEP and subsequently treated with the corresponding linker-payload<sup>11</sup> (LP) giving ADCs 1–6 (Scheme 1). The resulting ADC was buffer exchanged (diafiltration) into an appropriate buffer for the hydrolysis reaction (*vide infra*). Loading (DAR) and % succinimide hydrolysis were evaluated by LCMS of the fully reduced ADC. Owing to the nature of hinge conjugates, the linker-payload was partially loaded onto all exposed cysteine residues (3 on the heavy chain and 1 on the light chain). The progress of the hydrolysis reaction was monitored by careful observation of the conjugated light-chain species, as illustrated in Figure 3. The

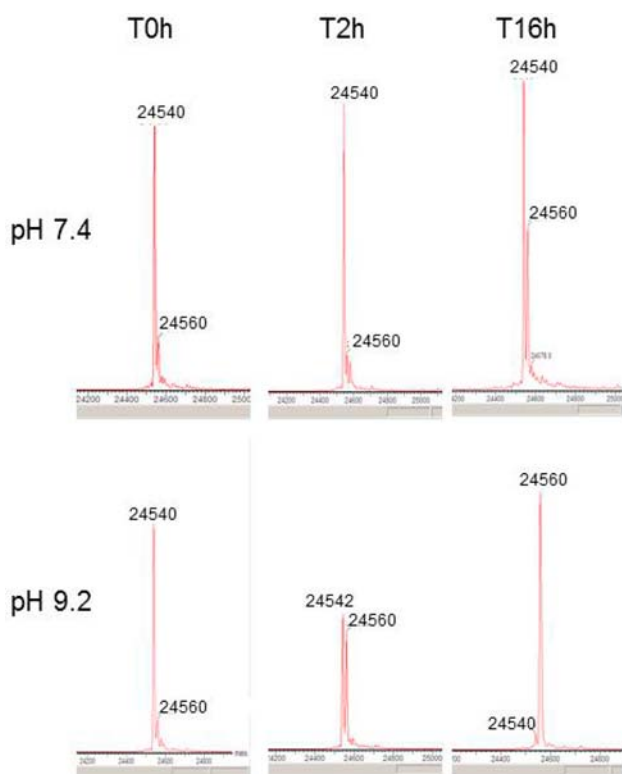


**Figure 3.** Tracking the progression of ring-opening of Tras\_Mal-Peg6C2\_Payload1 (1) by MS of the light chain.

unmodified light chain (MW = 23 422, not shown) was also present and was unchanged during the course of the described reaction. The conjugated light chain (LC+1LP) of Tras\_Mal-Peg6C2\_PayloadA (1) was observed to have an initial MW of 24 540, a mass shift of 1118 Da from the unconjugated LC. Over the course of the reaction, the 24 540 peak decreased in intensity, while a new peak at 24 560 grew in its place (Figure 3). This increase in mass of approximately 20 Da is almost certainly due to the intended succinimide hydrolysis. (Note that there is an error of  $\pm \sim 2$  Da in the MS analysis.) Only  $\sim 30\%$  conversion was observed after 16 h at pH 7.4, but the reaction was essentially complete after 14 h when performed at pH 9.2 (Figure 3 and Figure 4a). Importantly, the succinimide

rings on both heavy chains and light chains were shown to be hydrolyzed under these conditions. For example, Figure 5 shows the mass spectrum of the heavy and light chains both before (Figure 5A) and after (Figure 5B) hydrolysis. As expected, the MW of the unloaded heavy chain and light chain did not shift upon hydrolysis while the mass shift of the loaded heavy chains corresponded with the number of succinimides present. In other words, the HC+2 peak shifted approximately by the addition of two water molecules (36 Da) while the HC +3 peak shifted approximately by the addition of three water molecules (54 Da). With these conditions in hand, we proceeded to make three hydrolyzed succinimide Mal-Peg6C2-containing ADCs 1RO–3RO (Scheme 1 and Table S1, Supporting Information). In each case, the appropriate mass shift was observed for the initial conjugation and the mass shift increased by approximately 18 Da upon succinimide hydrolysis.

Hydrolysis of the mc-linked ADCs proved to be more challenging. No ring opening was observed at neutral pH, while at pH 8.5 and 9.2 the reaction only proceeded to 29% and 54% conversion, respectively, after 14 h of heating at 37 °C (Figure 4b). In order to drive the hydrolysis to completion, the reaction was heated to 45 °C for 48 h. Under these more forcing conditions, however, approximately 20–25% of the linker-payload was lost, presumably due to retro-Michael type reaction of the linker-payload followed by attack of hydroxide onto the resulting electrophile. Similar loss of MalPeg6C2 linker was observed but the milder conditions limited the loss to 10–15% (Table S1, Supporting Information). This loss of DAR can be mitigated by performing the hydrolysis reaction with ADC that has 20–25% higher DAR than the intended DAR of the final product. These optimized conditions (45 °C, pH 9.2, 48 h) were used to generate three hydrolyzed mc-linked ADCs (4RO–6RO) for further study (Scheme 1 and Table S1, Supporting Information). Each example showed the appropriate mass shift for the initial conjugate and a mass shift of approximately 18 Da/DAR upon hydrolysis of the succinimide ring. While the ADCs were generally stable to the reaction conditions, peptide mapping of 6RO revealed that the high pH conditions resulted in significant asparagine deamidation ( $\sim 70\%$ ) on the N30 residue (peptide sequence ASQDVNTAVAWYQQKPGKAPK). However, this change did not seem to have an effect on antigen binding (*vide infra*) and the ring-opening conditions did not appear to promote any significant changes in the overall structure of the ADC as measured by SEC, forced thermal aggregation, or DSC (data not shown).

#### Hydrolyzed Succinimide ADCs Are Potent and Selective for Antigen Expressing Cell Lines *in Vitro*.

The resulting six pairs of unhydrolyzed and hydrolyzed ADCs (1–6 and 1RO–6RO, respectively) were evaluated for *in vitro* cytotoxicity against a panel of Her2 expressing (N87 and BT474) and Her2 negative (MB468) cell lines. The results are summarized in Table 1. There was no significant difference between the corresponding hydrolyzed and unhydrolyzed ADCs. All ADCs, whether ring-opened or ring-closed, are potent against the Her2 expressing cell lines and are very weakly active against the nonexpressing cell lines. This indicates that the payload is being effectively delivered to the cells in an antigen-dependent manner, consistent with the well-established mode of action for ADCs. Additionally, the hydrolyzed and unhydrolyzed ADCs were found to bind to the Her2 antigen with approximately the same affinity as unmodified trastuzumab (Figure S1, Supporting Information).

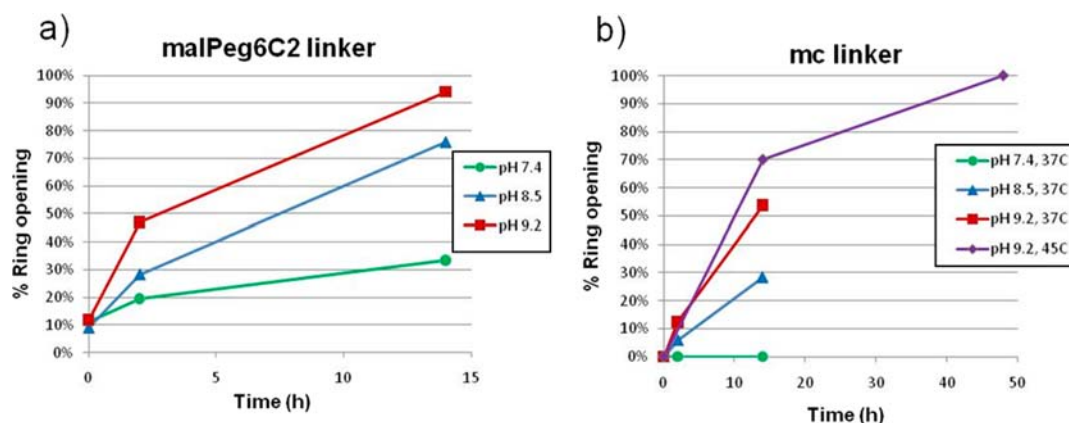


**Figure 4.** Kinetics of succinimide hydrolysis at various pH's for Tras\_MalPeg6C2\_PayloadA (1) (a) and Tras\_mc\_PayloadA (4) (b). Hydrolysis reactions were conducted at 37 °C, unless otherwise noted. Buffers used were 50 mM phosphate (pH 7.4), 50 mM borate (pH 8.5), and 50 mM borate (pH 9.2).

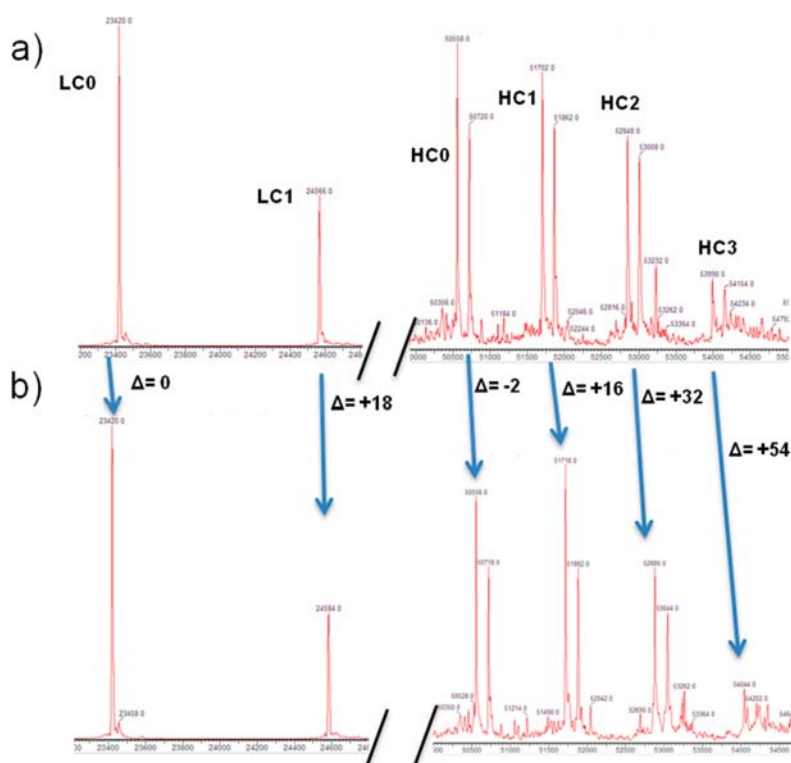


**Figure 5.** Mass spectrometry traces of (a) Tras\_MalPeg6C2\_PayloadC (3) and (b) hydrolyzed Tras\_MalPeg6C2\_PayloadC (3RO). The “doublet” peaks for the HC region are due to the presence of multiple glycoforms, differing by approximately 160 Da.

**Hydrolyzed Succinimide ADCs Show Improved *in Vitro* and *in Vivo* Stability.** Having established that the succinimide ring-opening reaction does not significantly impact ADC cytotoxicity, antigen binding, or thermal stability, we proceeded to evaluate the metabolic stability of the resulting antibody–toxin linkage. Two methods were employed in order to determine if succinimide hydrolysis prevented the retro-Michael mediated loss of payload from the ADC. First, the ADC was subjected to a large excess of a thiol (500  $\mu$ M glutathione) at pH 7.4 in order to promote the retro-Michael type reaction. The DAR was monitored by LCMS (under reducing conditions) over a 6 day period to see if succinimide hydrolysis would prevent or drastically slow the thiol-promoted linker-payload loss. Second, the ADC was incubated in mouse plasma in order to mimic the *in vivo* environment during an

efficacy study. The ADC was captured from the plasma with an immobilized anti-Fc reagent. After acid elution, the ADC was reduced (TCEP) and the DAR was evaluated. Since it had been previously demonstrated that the succinimide ring of the MalPeg6C2 ADCs spontaneously opens in solution, we expected the effect of hydrolysis to be more pronounced for mc-linked ADCs than for the MalPeg6C2 ADCs. Therefore, the focus of these stability studies and the subsequent *in vivo* studies was on the three mc-linked ADCs (4–6 and 4RO–6RO; Figure 6).

The unhydrolyzed ADCs (4–6) lost 30–60% of their loading (DAR) during the course of 6 days in the presence of 500  $\mu$ M glutathione (37 °C, pH 7.4) (Figure 6). Only fully loaded and unloaded LC and HC peaks were observed by MS, with no peaks observed for a retained linker stub or cleavage of



Table 1. *In Vitro* Potency for the 6 Pairs of ADCs<sup>a</sup>

		MalPeg6C2		Mc	
		ring closed (1–3)	ring opened (1RO–3RO)	ring closed (4–6)	ring opened (4RO–6RO)
Payload A	N87 (+++)	0.53	0.96	0.33	0.40
	BT474 (+++)	0.28	0.49	0.19	0.25
	MDA-MB-468 (–)	480	480	560	430
Payload B	N87 (+++)	2.1	5.8	3.7	1.5
	BT474 (+++)	0.48	0.83	0.45	0.40
	MDA-MB-468 (–)	770	460	>910	760
Payload C	N87 (+++)	NA	3.4	1.0	0.66
	BT474 (+++)	NA	1.1	0.33	0.40
	MDA-MB-468 (–)	NA	700	510	540

<sup>a</sup>IC<sub>50</sub> in nM, based on payload concentration. Note that compound 3 was not evaluated.

the payload, strongly suggesting that the primary mechanism of payload loss is retro-Michael type loss of the maleimide. The corresponding hydrolyzed ADCs (4RO–6RO) retained 90% or more of their loading (DAR) during the same time course, indicating that the ring-opened succinimide is unable to undergo the retro-Michael type reaction. Similarly, the ring-closed ADCs (4–6) lost 30–45% of their payload over a two-day period in mouse plasma (under a CO<sub>2</sub> atmosphere at 37 °C). Again, no intermediate peaks were observed indicating that the primary mechanism of loss is retro-Michael mediated. Interestingly, the majority of the DAR loss occurred within the first 24 h, after which time the rate of loss appears to have stabilized. This suggests that perhaps some hinge-cysteine sites may be more susceptible to payload loss than others. The hydrolyzed ADCs (4RO–6RO) all showed less than 10% loss of linker-payload during the same time period. *These results clearly show that ADCs that have undergone hydrolysis of the*

succinimide rings are resistant to both thiol-mediated and plasma-mediated loss of payload.

**anti-Her2 ADCs with Hydrolyzed Succinimide Rings Show Improved Pharmacokinetics (PK) Relative to the Unhydrolyzed ADCs.** Three pairs of ADCs were dosed at 3 mg/kg (mpk) to nontumor bearing mice, and plasma samples were collected at various time points over the course of a 14-day study. The total antibody (T<sub>ab</sub>) and ADC concentrations were determined by a ligand binding assay (LBA). Figure 7 illustrates the effects of succinimide ring hydrolysis on Tras<sub>mc</sub> PayloadB (5 vs 5RO). The AUC was improved, the ADC/T<sub>ab</sub> was increased, and the ADC clearance was decreased for the hydrolyzed version of this ADC (5RO). These trends were also observed for the remaining two pairs of ADCs, 4/4RO, and 6/6RO (Table 2). While the magnitude of the improvement was modest for each example, the trends were consistent for all three pairs of ADCs. One reason for the relatively modest improvement in AUC may be the well-known insensitivity of LBA to changes in DAR. In other words, payload may be lost from the ADC without a concomitant loss in LBA signal because the assay is known to be somewhat insensitive to changes in DAR. This is presumably due to steric obstruction that prevents the anti-payload reagent from binding to multiple payloads on the ADC simultaneously. With this in mind, one pair of ADCs (6/6RO) was evaluated for *in vivo* DAR loss by mass spectrometry (Figure 8). From this data, it is clear that the ring-opened ADC has improved retention of payload as compared to the ring-closed ADC.

**Anti-Her2 ADCs with Hydrolyzed Succinimide Rings Show Improved *in Vivo* Efficacy Relative to the Unhydrolyzed ADCs.** The three pairs of ADCs were dosed at 1, 3, and 10 mpk in a mouse xenograft model using an N87 gastric tumor line. Dosing was performed qdx4, on days 1, 5, 9, and 13. Eight animals were used in each dosing group and a PBS vehicle group was run in each study as a negative control. The 10 mpk dose resulted in complete tumor suppression in nearly every example and was therefore not useful in drawing

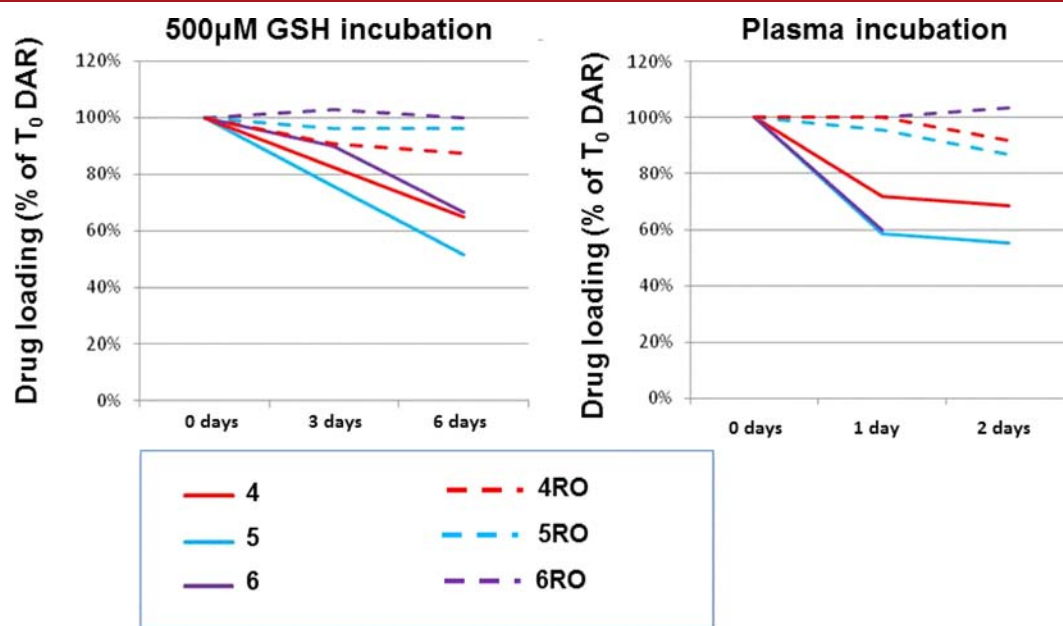


**Figure 6.** Stability studies for 4–6 (solid lines) and 4RO–6RO (dashed lines) in 500 µM glutathione (left) and mouse plasma (right). The loading is expressed relative to the T<sub>0</sub> DAR. Raw loading values are shown in Table S2 (Supporting Information).

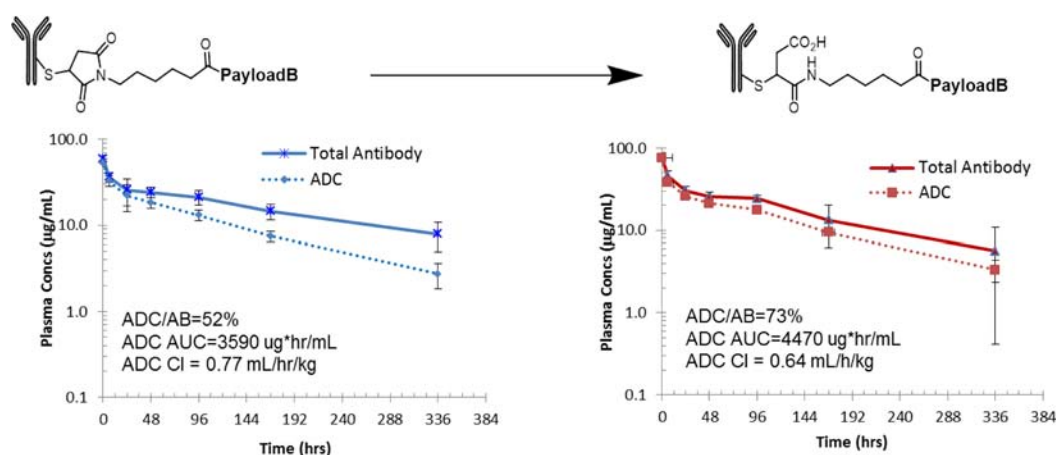


**Figure 7.** PK of compounds **5** and **5RO** (mouse, 3mpk) showing that succinimide ring-opening improves AUC, ADC/ $T_{Ab}$ , and Cl. Tabular results for all 6 ADCs can be found in Table 2.

**Table 2.** PK Data for the 6 Comparator ADCs Illustrating that Succinimide Ring-Opening Results in Increased AUC, Improved ADC/ $T_{Ab}$ , and Decreased Clearance

		DAR	ADC AUC ( $\mu\text{g h/mL}$ )	ADC Cl ( $\text{mL/h/kg}$ )	ADC $T_{1/2}$ (days)	$T_{Ab}$ $T_{1/2}$ (days)	ADC AUC/ $T_{Ab}$ AUC
mc_PayloadA	Ring closed ( <b>4</b> )	4.1	2160 $\pm$ 510	1.38	2.7	4.4	55%
	Ring opened ( <b>4RO</b> )	3.4	3490 $\pm$ 710	0.77	5.7	7.2	65%
mc_PayloadB	Ring closed ( <b>5</b> )	3.4	3590 $\pm$ 600	0.77	4.4	7.1	52%
	Ring opened ( <b>5RO</b> )	3.6	4470 $\pm$ 1100	0.64	4.5	5.2	76%
mc_PayloadC	Ring closed ( <b>6</b> )	4.0	1930 $\pm$ 420	1.48	3.0	5.2	58%
	Ring opened ( <b>6RO</b> )	4.0	2330 $\pm$ 640	1.21	3.6	4.4	68%

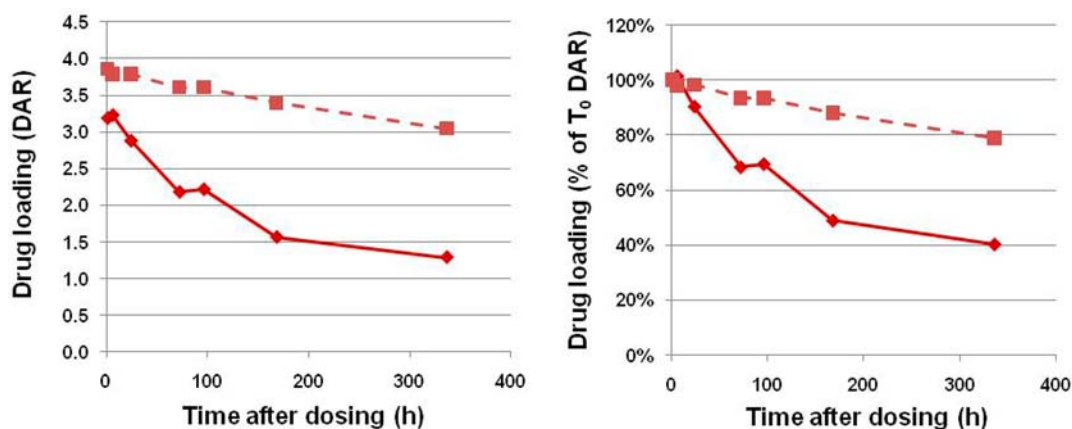


**Figure 8.** DAR analysis of **6** (solid line) and **6RO** (dashed line) at various time points following a 3mpk administration to mice. Data on the left is the raw DAR values and data on the right is normalized to  $T_0$  DAR.

comparisons between the hydrolyzed and unhydrolyzed ADCs. However, the 3 mpk dose of **4RO** and **5RO** slightly outperformed the corresponding ring-closed ADCs **4** and **5** (Figure 9A,B). Interestingly, compound **6RO** clearly outperformed the corresponding ring-closed ADC **6** at this dose (Figure 9C). The ring opened ADC **6RO** resulted in complete tumor regression for 4 animals and partial regression and stasis for the remaining 4 animals when dosed at 3 mpk (Figure S2, Supporting Information). In contrast, the corresponding unhydrolyzed ADC **6** caused complete regression in 3 animals but temporary regression followed by uncontrolled tumor growth in the remaining 5 animals.

The 1mpk dose of **4RO** and **6RO** also outperformed ring-closed succinimides **4** and **6**, respectively. The difference observed between **4** and **4RO** was particularly dramatic at this

dose, showing that the ring-closed version (**4**) had essentially no activity as compared to vehicle while the ring-opened version (**4RO**) resulted in tumor stasis. The stark difference between these two ADCs is also clearly evident in the waterfall plot shown in Figure 9D. The improvement in efficacy that was observed upon ring-opening for these ADCs does not appear to be driven by the slight differences in initial DAR (Table 2).

## DISCUSSION AND CONCLUSIONS

The limited stability of maleimide linked payloads on ADCs was first noted in 2005 by Wahl, who found that the DAR of an anti-CD30 vcMMAE conjugate dosed in mice dropped from  $\sim 4.8$  at  $T_0$  to  $\sim 1.8$  at 9 days.<sup>12</sup> The DAR analysis was performed using an ELISA-based assay, so it was unclear at the time whether the loss of DAR was due to cathepsin-mediated

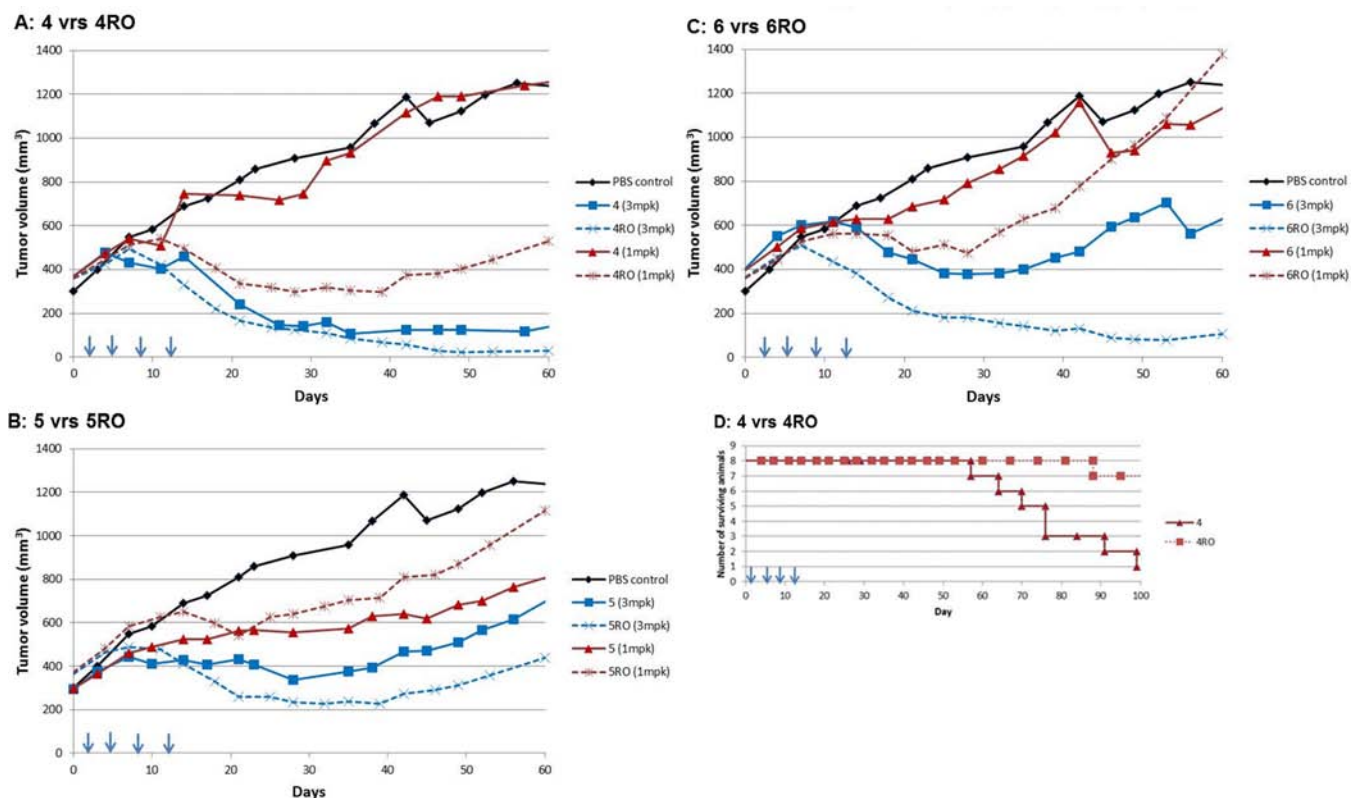


**Figure 9.** Tumor xenograft data for compounds **4** and **4RO**, **5** and **5RO**, and **6** and **6RO** (panels A, B, and C, respectively) in an N87 xenograft model. Solid lines are ring-closed ADCs (**4**–**6**) and dashed lines are ring-opened ADCs (**4RO**–**6RO**). Panel D is a waterfall plot of compounds **4** and **4RO** at 1 mpk.

cleavage of the ValCit linker or to some other mechanism (such as maleimide transfer). The liabilities of maleimide-linked ADCs became more clear in 2008 when the same group conducted a related study of an anti-CD70 vcMMAE conjugate in which the maleimide electrophile was replaced by a bromoacetamide.<sup>7</sup> The bromoacetamide-based ADC was far more stable than the corresponding maleimide-based ADC, clearly showing that the primary metabolic pathway for loss of this linker-payload is retro-Michael mediated, whereby the payload is ultimately transferred to cys-34 of serum albumin. The transfer of maleimides from antibodies to serum albumin has been confirmed by other reports<sup>9,13</sup> and the mechanism of transfer has been studied in some detail.<sup>8</sup> Unexpectedly, bromoacetamide conjugation resulted in improved stability but did not result in improvements in efficacy.<sup>7</sup> The authors speculate that improvement of the linker half-life beyond the half-life of the ADC itself offers little *in vivo* benefit.

Results from our study shed additional light on the relationship between ADC stability and efficacy. Six maleimide ADCs (**1**–**6**) were prepared and were directly compared to the corresponding ring-opened ADCs (**1RO**–**6RO**). The change in the linker did not affect the potency or selectivity of the ADCs in various *in vitro* cytotoxicity models (Table 1). However, the ADCs with hydrolyzed succinimide rings showed a significant improvement in stability in a thiol-promoted deconjugation assay and a plasma stability assay (Figure 5). This improved stability was found to translate to improved PK exposure and improved ADC/Ab ratios in LBA-based PK studies when compared to the parent ADCs where the succinimide rings were intact (Figure 7 and Table 2). One pair of compounds (**6** and **6RO**) was evaluated in a MS based

PK study in which the ADC was captured on immobilized anti-Fc resin, eluted, deglycosylated, reduced, and evaluated for loading (Figure 8). This study showed that the linker half-life for the unhydrolyzed ADCs was approximately 7 days, in line with previous reports.<sup>7</sup> The linker half-life for the ring-opened ADCs was >2 weeks. In no case was any linker stub observed, strongly suggesting that the primary mechanism of payload loss is simple retro-Michael type elimination of the maleimide.

While the trends shown in Figure 7 and Table 2 indicate that hydrolysis of the succinimide rings leads to improved stability, the question remains why the ADC/ $T_{Ab}$  did not approach 100% for the hydrolyzed ADCs (**4RO**–**6RO**). The fact that the ADC/ $T_{Ab}$  is in the range of 65–75% suggests that the DAR of the hydrolyzed ADCs is dropping over time. This was unexpected given the excellent stability in plasma and glutathione (Figure 5). Indeed, when the plasma samples from the PK study were analyzed by LCMS, it became clear that the LBA results did not present a complete picture of the fate of the payload. Figure 8 shows that the loading of ADC **6** decreases from ~3.3 at the initial time point to ~1.3 at the final time point—a decline of nearly 60%—while the hydrolyzed version of this ADC (**6RO**) loses only about 20% of its linker-payload during the same time period. While this is clearly an improvement, the question remains why the hydrolyzed ADC is losing any payload at all given the stability results illustrated in Figure 6. One possibility is that the hydrolyzed ADC may undergo a retro-Michael type mediated loss of payload, albeit at a slower rate than the ring-closed ADC. However, this seems highly unlikely given that Küick<sup>8</sup> reports that no glutathione exchange was observed for a ring-opened model compound over the course of a 7 day NMR study. Therefore, a more likely



explanation is that the higher loaded species (DAR6 and DAR8) are being more quickly cleared from the bloodstream than the lower loaded species. This is consistent with previous reports showing that high-DAR species of cAC10-vcMMAE were cleared more quickly than the lower DAR species.<sup>14</sup> The net result of this differential clearance is a time-dependent drop in DAR. Therefore, the net loss of payload for ADCs (4–6) is presumably a result of both retro-Michael type loss of payload and differential clearance of higher loaded species. It is interesting to note that site-specific ADCs would not be subject to payload loss via differential clearance since the ADC would be homogeneous. Thus, complete DAR retention may only be possible with homogeneous site-specific conjugates. Nevertheless, the improvement in stability afforded by succinimide hydrolysis of hinge conjugates is very clearly demonstrated in Figures 5–8 and prompted us to consider whether the improvement in stability would translate to an improvement in efficacy.

The ring-opened ADCs **4RO**–**6RO** in the present study generally showed a significant improvement in efficacy as compared to their ring-closed counterparts (**4**–**6**) (Figure 9). This observation is consistent with a report showing that site-specific conjugates with improved linker stability exhibit improved efficacy.<sup>9</sup> The present study of ADCs with hydrolyzed succinimide rings offers a way to similarly improve the linker stability and efficacy of conventional (hinge) cysteine conjugates. The improvement in efficacy seems to correlate modestly well with the improvement in ADC exposure as measured by LBA (Table 2). Interestingly, the best improvement in efficacy is observed for compounds **4RO** and **6RO**, both of which show a significant improvement in the ADC  $T_{1/2}$  as compared to their ring-closed counterparts **4** and **6**. ADC **5RO** shows a minimal improvement in efficacy, which appears to correspond with the nominal improvement in ADC  $T_{1/2}$ . In contrast to the previously published report,<sup>7</sup> our study shows that improvement in linker stability beyond the half-life of the ADC may, in fact, have a beneficial effect on efficacy. In the present study the linker half-life was improved from ~7 days (**6**) to >14 days (**6RO**) and a significant improvement in efficacy was observed in spite of an ADC half-life of ~3 days in mice.

Importantly, the improvement in efficacy for compound **6RO** did not come at the expense of decreased safety. Compounds **6** and **6RO** did not show any adverse events during the mouse efficacy study. Both compounds were dosed in rats and the cNOAEL was found to be 30 mpk for both compounds. The improvement in efficacy and the unchanged safety profile suggests that the ring-opened ADCs may offer an advantage in terms of therapeutic index (TI).

In summary, we have described a method for the preparation of succinimide ring-hydrolyzed conventional (hinge) conjugated ADCs. These ADCs show equivalent *in vitro* potency, improved *in vitro* stability, improved PK exposure, and improved efficacy as compared to their unhydrolyzed counterparts. This method offers a pathway to improve the stability and efficacy of maleimide linked linker-payloads without resorting to antibody engineering. Moreover, the improvement in efficacy that we report provides further justification for many of the maleimide replacement strategies that are currently being pursued.<sup>15</sup> In spite of promising *in vitro* results, few of these maleimide replacements have been thoroughly compared to the corresponding maleimide-linked ADC to see if they offer any advantage in terms of efficacy and/or safety. Our results

strongly suggest that maleimide replacements offer a clear opportunity for ADC optimization.

## MATERIALS AND METHODS

**Maleimide Conjugation Protocol.** Commercially available HERCEPTIN antibody (Genentech Inc.) was dialyzed into Dulbecco's Phosphate Buffered Saline (DPBS, Lonza). The dialyzed antibody was diluted to 15 mg/mL with PBS containing 5 mM 2,2',2'',2'''-(ethane-1,2-diylidinitrilo)tetraacetic acid (EDTA), pH 7. The resulting antibody was treated with 2–2.5 equiv of tris(2-carboxyethyl)phosphine hydrochloride (TCEP, 5 mM in distilled water) and allowed to stand 37 °C for 1–2 h. Upon cooling to rt, dimethylacetamide (DMA) was added to achieve 10% (v/v) total organic. The mixture was treated with 8–10 equiv of the appropriate linker-payload as a 10 mM stock solution in DMA. The reaction was allowed to stand for 1–2 h at rt and then buffer exchanged into DPBS (pH 7.4) using GE Healthcare Sephadex G-25 M buffer exchange columns per manufacturer's instructions. Material used for succinimide ring hydrolysis was immediately carried into the protocol outlined below. Material that was intended to remain ring-closed was purified by size exclusion chromatography (SEC) using GE AKTA Explorer system with a GE Superdex200 column and PBS (pH 7.4) eluent. Final samples were concentrated to ~5 mg/mL protein, filter sterilized, and checked for loading using the MS conditions outlined below.

**Succinimide Hydrolysis Protocol.** The antibody–drug conjugate obtained from the maleimide coupling above was immediately buffer exchanged into a 50 mM borate buffer (pH 9.2) using an ultrafiltration device (50 kD MW cutoff). The resulting solution was heated to either 37 °C for 24 h (for the maleimide-Peg linkers) or to 45 °C for 48 h (for the maleimide-caproyl linkers). The resulting solution was cooled, buffer-exchanged into PBS, and purified by SEC (as described previously) in order to remove any aggregated material. Final samples were concentrated to ~5 mg/mL protein, filter sterilized, and checked for DAR using the MS conditions outlined below.

**ADC Mass Spectrometry Studies.** Waters MicromassZQ mass spectrometer (ESI ionization; cone voltage: 20 V; Source temp: 120 °C; Desolvation temp: 350 °C). The crude spectrum containing the multiple-charged species was deconvoluted using MaxEnt1 within MassLynx 4.1 software package according to the manufacturer's instructions. The extent of succinimide ring hydrolysis was determined by examining the LC+1LP peak at ~24 kD.

**Forced Deconjugation Protocol.** ADC samples were diluted into aqueous glutathione (Sigma-Aldrich, St. Louis, MO) to yield a final GSH concentration of 0.5 mM and final protein concentration of ~3 mg/mL in a phosphate buffer, pH 7.4. The samples were then incubated at 37 °C and aliquots were removed at three time points to determine the DAR (T-0, T-3day, T-6day). The aliquot from each time point was treated with TCEP and analyzed by LC-MS. Liquid chromatography mass spectrometry (LC-MS) analysis was performed using a Waters Xevo Q-TOF G2 mass spectrometer (Waters, Milford, MA) coupled to an Agilent (Santa Clara, CA) 1100 capillary HPLC. The reduced samples were separated over an Agilent Poroshell 300SB-C8 (1.0 × 75 mm) column maintained at 80 °C with a flow rate of 65  $\mu$ L/min. Mobile phase A was water with 2% acetonitrile and 0.1% formic acid, and mobile phase B was acetonitrile with 2% water and 0.1% formic acid. Proteins were eluted from the column using a gradient: 2% to 20% B in



0.5 min, 20% to 40% B in 6 min, and 40% to 100% B in 4 min. The mass spectrometer was run in positive MS only mode scanning from 800 to 2000  $m/z$  and data was acquired with MassLynx (Waters) 4.1 software. The TOF-MS signal corresponding to the light and heavy chains were summarized and deconvoluted using MaxEnt1 (Waters) program.

**Cytotoxicity Assay.** All cell lines were obtained from ATCC (Manassas, VA). N87 originated from a liver metastasis of a colon carcinoma patient, and BT474 and MDA-MB-468 were derived from breast cancers. Cells were maintained in RPMI or DMEM media plus 10% bovine serum albumin and other supplements as recommended by ATCC. Cells were seeded in 96-well plates at low density, then treated the following day with compounds at 3-fold serial dilutions at 10 concentrations in duplicate. Cells were incubated for 4 days in a humidified 37 °C/5% CO<sub>2</sub> incubator. The plates were harvested by incubating with CellTiter 96 AQueous One MTS Solution (Promega, Madison, WI) for 1.5 h and absorbance measured on a Victor plate reader (PerkinElmer, Waltham, MA) at wavelength 490 nm. IC<sub>50</sub> values were calculated using a four-parameter logistic model with XLfit (IDBS, Bridgewater, NJ).

**Plasma Stability Protocol.** ADC samples (~1.5 mg/mL) were diluted into mouse plasma (Lampire Biological Laboratories, Pipersville, PA) to yield a final solution of 10% ADC, 90% plasma. Samples were incubated under a CO<sub>2</sub> atm and aliquots were removed at three time points to determine their DAR (T-0 h, T-24 h, and T-48 h). Each time point underwent an immunoprecipitation process to enrich the ADC. Briefly, each aliquot was diluted 1:1 in 20% MPER (Thermo Fisher Scientific, Waltham, MA) and equal amounts of biotinylated mouse anti-human Fc and goat anti-human kappa antibodies (SouthernBiotech, Birmingham, AL) were added. The samples were incubated for 2 h at 4 °C followed by the addition of streptavidin Dynabeads (Thermo Fisher Scientific). Samples were processed on a KingFisher instrument with four washing steps consisting of 10% MPER, 0.05% Tween 20, and twice with PBS. The ADC was eluted off the beads with 0.15% formic acid. Samples were pH adjusted to 7.8 with 2 M Tris pH 8.5 and their N-linked glycans were removed with PNGaseF (New England Biolabs, Ipswich, MA). The samples were reduced with TCEP and analyzed by LC-MS as described in Forced Deconjugation Protocol.

**PK Protocol.** Non-tumor-bearing athymic female nu/nu (nude)mice (6–8 weeks of age) were obtained from Charles River Laboratories, Wilmington, MA, USA. All procedures using mice were approved by the Institutional Animal Care and Use Committee according to established guidelines. Mice ( $n = 3$  or 4) were administered a single intravenous dose of an ADC at 3 mg/kg based on the antibody component. Blood samples were collected from each mouse via the tail vein at 0.083, 6, 24, 48, 96, 168, and 336 h postdose. The total antibody ( $T_{ab}$ ) and ADC concentrations were determined by a LBA where a sheep antihuman IgG antibody (Binding Site, San Diego, CA, USA) was used for capture, a goat antihuman IgG antibody (Bethyl Laboratories, Inc., Montgomery, TX, USA) was used for detection of  $T_{ab}$  or an anti-payload antibody (Pfizer, Inc.) was used for detection of ADC. Plasma concentration data for each animal was analyzed using Watson LIMS v 7.4 (Thermo).

**In Vivo DAR Analysis.** The ADC samples were deglycosylated by treating with PNGase (New England Biolab) at 37 °C for 1 h. Following the incubation, a capture antibody (biotinylated goat anti-human Fc at 1.0 mg/mL, Jackson

ImmunoResearch) was added and the mixture was heated at 37 °C for 1 h followed by gentle shaking at room temperature for a second hour. Dynabead MyOne Streptavidin T1 beads (Invitrogen) were added to the samples and incubated at rt for at least 30 min while gently shaking. The sample plate was then washed with 200  $\mu$ L PBS + 0.05% Tween 20, 200  $\mu$ L PBS, and HPLC grade water. The bound ADC was eluted with 55  $\mu$ L 2% of formic acid (v/v). Fifty microliter aliquots of each sample were transferred into a new plate followed by an additional 5  $\mu$ L of 200 mM TCEP.

The intact protein analysis was carried out with Xevo G2 QToF mass spectrometer (Waters, Manchester, UK) coupled with Nano Acquity (waters) and BEH300 C<sub>4</sub>, 1.7  $\mu$ m, 0.3  $\times$  100 mm column (Waters), using MassLynx v 4.1 as acquisition software. The column temperature was set at 85 °C. Mobile phase A consisted of 0.1% TFA (trifluoroacetic acid) in water. Mobile phase B consisted of 0.1% TFA in acetonitrile:1-propanol (1:1, v/v). The chromatographic separation was achieved at a flow rate of 18  $\mu$ L/min using a linear gradient of mobile phase B from 5% to 90% over 7 min.

Data analysis including deconvolution was performed using Biopharmalynx v 1.33 (Waters). The following equation was used for average DAR calculation:

$$\begin{aligned}\text{Average DAR} = & (LC1/(LC0 + LC1)) \times 2 \\ & + (HC1/(HC0 + HC1 + HC2 + HC3)) \times 2 \\ & + (HC2/(HC0 + HC1 + HC2 + HC3)) \times 4 \\ & + (HC3/(HC0 + HC1 + HC2 + HC3)) \times 6\end{aligned}$$

where LC0 and LC1 is the intensity (AUC) of the signal for the light chain with zero and one payloads, respectively, and HC0, HC1, HC2, and HC3 is the intensity (AUC) of the signal for the heavy chain with 0, 1, 2, 3 payloads, respectively.

**In Vivo Efficacy Study.** *In vivo* efficacy studies of antibody–drug conjugates were performed in a target-expressing xenograft model using the N87 cell line. Approximately 7.5 million tumor cells in 50% matrigel were implanted subcutaneously into 6–8 weeks old nude mice until the tumor sizes reach between 250 and 350 mm<sup>3</sup>. The drug was dosed through bolus tail vein injection. Animals were injected with 10, 3, or 1 mg/kg of antibody drug conjugate a total of four times, once every 4 days (on days 1, 5, 9, and 13). All experimental animals are monitored for body weight changes weekly. Tumor volume is measured twice a week for the first 50 days and once weekly thereafter by a caliper device and calculated with the following formula: Tumor volume = (length  $\times$  width<sup>2</sup>)/2. Animals are humanely sacrificed before their tumor volumes reach 2500 mm<sup>3</sup>. The tumor size is generally observed to decrease after the first week of treatment. Animals were monitored continuously for tumor regrowth after the treatment has discontinued (up to 100 days post-treatment).

## ■ ASSOCIATED CONTENT

### Supporting Information

Table S1: Mass shifts and DAR loss during succinimide hydrolysis. Table S2: Raw loading values (DAR) for glutathione stability and plasma stability studies. Figures illustrating binding affinity and tumor volume data. This material is available free of charge via the Internet at <http://pubs.acs.org>.

## ■ AUTHOR INFORMATION

## Corresponding Author

\*E-mail: Nathan.Tumey@pfizer.com.

## Notes

The authors declare no competing financial interest.

## ■ ACKNOWLEDGMENTS

The authors would like to thank Andreas Maderna, Matt Doroski, and Alex Porte for designing and supplying the linker-payloads needed for this study, My-Hanh Lam and Sylvia Musto for running the in vitro cytotoxicity assays, Sadhana Jain and Mark Krebs for performing ADC physical stability studies, Kathleen Pelletier and JoAnn Wentland for technical support in the PK studies, and Chris O'Donnell for helpful advice, managerial support, and manuscript editing.

## ■ REFERENCES

- (1) Beck, A., and Reichert Janice, M. (2014) Antibody-drug conjugates: present and future. *mAbs* 6 (1), 15–7.
- (2) (a) Sassoon, I., and Blanc, V. (2013) Antibody-drug conjugate (ADC) clinical pipeline: a review. *Methods Mol. Biol.* 1045, 1–27. (b) Perez, H. L., Cardarelli, P. M., Deshpande, S., Gangwar, S., Schroeder, G. M., Vite, G. D., and Borzilleri, R. M. (2014) Antibody-drug conjugates: current status and future directions. *Drug Discovery Today* 19 (7), 869–881.
- (3) (a) Gualberto, A. (2012) Brentuximab Vedotin (SGN-35), an antibody-drug conjugate for the treatment of CD30-positive malignancies. *Expert Opin. Invest. Drugs* 21 (2), 205–216. (b) Ballantyne, A., and Dhillon, S. (2013) Trastuzumab emtansine: first global approval. *Drugs* 73 (7), 755–765.
- (4) Hamann, P. R., Hinman, L. M., Hollander, I., Beyer, C. F., Lindh, D., Holcomb, R., Hallett, W., Tsou, H.-R., Upeslaci, J., Shochat, D., Mountain, A., Flowers, D. A., Bernstein, I., and Gemtuzumab Ozogamicin, A. (2002) Potent and selective anti-CD33 antibody-calicheamicin conjugate for treatment of acute myeloid leukemia. *Bioconjugate Chem.* 13 (1), 47–58.
- (5) Boghaert, E. R., Khandke, K. M., Sridharan, L., Dougher, M., DiJoseph, J. F., Kunz, A., Hamann, P. R., Moran, J., Chaudhary, I., and Damle, N. K. (2008) Determination of pharmacokinetic values of calicheamicin-antibody conjugates in mice by plasmon resonance analysis of small (5  $\mu$ l) blood samples. *Cancer Chemother. Pharmacol.* 61 (6), 1027–1035.
- (6) Xie, H., Audette, C., Hoffee, M., Lambert, J. M., and Blaettler, W. A. (2004) Pharmacokinetics and biodistribution of the antitumor immunoconjugate, cantuzumab mertansine (huC242-DM1), and its two components in mice. *J. Pharmacol. Exp. Ther.* 308 (3), 1073–1082.
- (7) Alley, S. C., Benjamin, D. R., Jeffrey, S. C., Okeley, N. M., Meyer, D. L., Sanderson, R. J., and Senter, P. D. (2008) Contribution of linker stability to the activities of anticancer immunoconjugates. *Bioconjugate Chem.* 19 (3), 759–765.
- (8) Baldwin, A. D., and Kiick, K. L. (2011) Tunable degradation of maleimide-thiol adducts in reducing environments. *Bioconjugate Chem.* 22 (10), 1946–1953.
- (9) Shen, B.-Q., Xu, K., Liu, L., Raab, H., Bhakta, S., Kenrick, M., Parsons-Reponte, K. L., Tien, J., Yu, S.-F., Mai, E., Li, D., Tibbitts, J., Baudys, J., Saad, O. M., Scales, S. J., McDonald, P. J., Hass, P. E., Eigenbrot, C., Nguyen, T., Solis, W. A., Fujii, R. N., Flagella, K. M., Patel, D., Spencer, S. D., Khawli, L. A., Ebens, A., Wong, W. L., Vandlen, R., Kaur, S., Shiwkowski, M. X., Scheller, R. H., Polakis, P., and Junutula, J. R. (2012) Conjugation site modulates the in vivo stability and therapeutic activity of antibody-drug conjugates. *Nat. Biotechnol.* 30 (2), 184–189.
- (10) Stefano James, E., Busch, M., Hou, L., Park, A., and Gianolio Diego, A. (2013) Micro- and mid-scale maleimide-based conjugation of cytotoxic drugs to antibody hinge region thiols for tumor targeting. *Methods Mol. Biol.* 1045, 145–71.
- (11) Doroski, M. D.; Maderna, A.; O'Donnell, C. J.; Subramanyam, C.; Vetelino, B. C.; Dushin, R. G.; Strop, P.; Graziani, E. I. (Pfizer) Cytotoxic peptides and antibody drug conjugates thereof. Pat. Appl. No. WO 2013/072813 A2, reference document 20121107, May 23, 2013.
- (12) Sanderson, R. J., Hering, M. A., James, S. F., Sun, M. M. C., Doronina, S. O., Siadak, A. W., Senter, P. D., and Wahl, A. F. (2005) In vivo drug-linker stability of an anti-CD30 dipeptide-linked auristatin immunoconjugate. *Clin. Cancer Res.* 11, 843–852.
- (13) Jackson, D., Atkinson, J., Guevara, C. I., Zhang, C., Kery, V., Moon, S.-J., Virata, C., Yang, P., Lowe, C., Pinkstaff, J., Cho, H., Knudsen, N., Manibusan, A., Tian, F., Sun, Y., Lu, Y., Sellers, A., Jia, X.-C., Joseph, I., Anand, B., Morrison, K., Pereira, D. S., and Stover, D. (2014) In vitro and in vivo evaluation of cysteine and site specific conjugated herceptin antibody-drug conjugates. *PLoS One* 9 (1), e83865/1–e83865/14 14 pp.
- (14) Hamblett, K. J., Senter, P. D., Chace, D. F., Sun, M. M. C., Lenox, J., Cervený, C. G., Kissler, K. M., Bernhardt, S. X., Kopcha, A. K., Zabinski, R. F., Meyer, D. L., and Francisco, J. A. (2004) Effects of drug loading on the antitumor activity of a monoclonal antibody drug conjugate. *Clin. Cancer Res.* 10 (20), 7063–7070.
- (15) (a) Toda, N., Asano, S., and Barbas, C. F., III (2013) Rapid, stable, chemoselective labeling of thiols with Julia-Kocienski-like reagents: A serum-stable alternative to maleimide-based protein conjugation. *Angew. Chem., Int. Ed.* 52 (48), 12592–12596. (b) Badescu, G., Bryant, P., Swierkosz, J., Khayrabad, F., Pawlisz, E., Farys, M., Cong, Y., Muron, M., Rumpf, N., Brocchini, S., and Godwin, A. (2014) A new reagent for stable thiol-specific conjugation. *Bioconjugate Chem.* 25 (3), 460–469. (c) Lyon, R., Setter, J., Bovee, T., Doronina, S., Hunter, J., Anderson, M., Balasubramanian, C., Duhino, S., Lieske, C., Li, F., and Senter, P. (2014) Self-stabilizing maleimides improve the stability and pharmacological properties of antibody-drug-conjugates. *Nat. Biotechnol.*